

# Investigations on the Controllability and the Design of DC/DC Converters connected to PV – Generators

C.P. DICK, K. RIGBERS, H. RADERMACHER and R.W. De DONCKER

RWTH Aachen University, Germany

**Summary: Abstract—** This paper presents analytical and computer aided investigations on photovoltaic (PV) - generators connected to DC/DC converters for module integrated inverters. It shows the controllability and describes how to design the converters regarding requirements such as a wide variable input voltage range, a constant output voltage and a variable transferred power, depending on temperature, solar radiation and the PV-generator itself. Due to the high non-linearity of the PV-generator’s characteristic, a mathematic model is presented in a basic form and it is applied to several real systems showing the controllability and important information on the design.

**Key words:** DC-DC power conversion, photovoltaics, renewables

## 1. INTRODUCTION

The photovoltaic (PV) generator’s maximum power point (MPP) voltage varies depending on solar radiation and temperature within a ratio of 1:2 [1]. Connecting PV-modules in series to strings, the minimum MPP voltage of the PV-generator can be increased above the minimum required voltage level for feeding energy into the mains. The highest efficiency of PV-converters, only regarding the converter, is nowadays reached by the one-stage HERIC topology [2], basically consisting of an H-Bridge. Due to the high variation of the input voltage, the converter has consequently to be designed for a dc-link voltage  $U_{dc}$  more than twice as high as the minimum level for feeding the mains. Hence, the implemented high voltage switching devices show a high on-state resistance resulting in a poor efficiency in case of a low input voltage.

Module integrated PV-converters, which are expected to realize a higher overall system efficiency compared to string or central systems, have a minimum of two power stages, thus offering more flexibility for the dc voltage control (cmp. Fig. 1.)

In contrast to the HERIC topology, the grid-feeding DC/AC converter is not oversized and is working on the constant minimum voltage level  $U_{dc}$  for feeding mains. The first power stage consists of a DC/DC converter and adapts the variable input voltage  $U_{in}$  to  $U_{dc}$ . In this paper it is assumed that the second power stage, the DC/AC converter, is current controlled in the fastest control loop. The second control loop adapts the peak value of the current in order to control the dc-link voltage  $U_{dc}$  to a constant value. Thus, the DC/DC converter is clamped at its output. In a third, slow control loop the first power stage can perform maximum power point tracking (MPPT).

Regarding the DC/DC converter, there are several suitable topologies for handling the varying input voltage and power. This paper describes the module integrated converter system consisting of the PV-module and the DC/DC converter clamped to a constant output voltage. Together with the fundamentals of these two components an idealized analytical approach is presented. Subsequently, this approach is applied

to real systems, using a mathematic tool for solving the transcendent problems arising with the non-linear characteristic of PV-generators.

## 2. FUNDAMENTALS

The analyzed system consists of a PV-generator and a DC/DC converter with a fixed output voltage. The PV-generator can be modelled with the Shockley equation for Diodes. Together with datasheets of PV-modules this equation is over determined by one parameter. Thus, a linear term is added and the PV-module is modelled by:

$$I(U_{in}) = I_{SC} - I_0 \left( e^{\frac{U_{in}}{U_0}} - 1 \right) - M U_{in} \quad (1)$$

with  $I$ , PV-generator current;  $I_{SC}$ , PV-generator short circuit current;  $I_0$  and  $U_0$ , parameters and  $M \neq 0$ , additional parameter to the Shockley model. With the datasheets information on open circuit voltage,  $I_{SC}$ , MPP voltage and MPP current, a parameter-fitting process was carried out.

Taking additional information on temperature- and solar radiation dependencies into account, the PV-generator’s characteristic can be plotted for different operating points. Thereby, the illustration of the PV-generators power  $P_{PV}$  is mathematically equivalent to the illustration of current and useful in the discussion of MPPT.

Figure 2 shows the characteristics of one exemplary PV-module with, for example, curve D producing 165 W at a temperature of 25°C and a solar radiation of 1000 W/m<sup>2</sup>, being

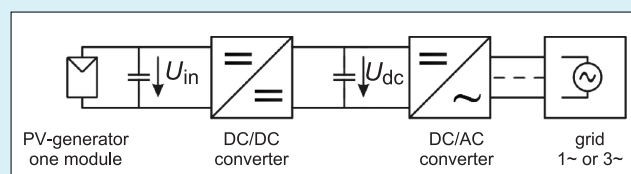


Fig. 1. Module Integrated Photovoltaic Inverter

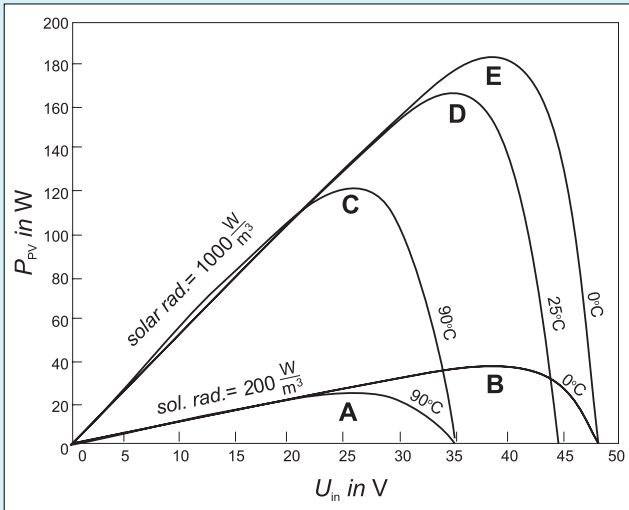


Fig. 2. Characteristics of the PV-Module Shell PowerMax™ Ultra 165

the standard test conditions. The other curves display maximum and minimum operating points for temperature [3]. Solar radiation can exceed the plotted operating points, but the plotted values of radiation are the boundaries of the most likely operating points.

The DC/DC converter has to handle all these operating points. Thus, the specifications become a variable voltage to voltage ratio, a variable transferred power and the ability to perform MPPT. Series resonant converters are not considered

since they have a fixed input-voltage to output-voltage ratio. The following topologies all contain a transformer to increase the voltage level. A detailed description can be found in the references [4, 5]. The most important information for this work are depicted in table I.

The transformer's leakage inductance  $L$  and the transformer's turns ratio  $U_{dc}/U'_{dc}$  can be chosen once in the design. One important controllable quantity in the analysis of the topologies is the converters switching frequency  $f$ . Table I gives an overview of suitable topologies.

### 3. IDEALIZED ANALYTICAL APPROACH

For an idealized analytical calculation the PV-generators characteristic and the transferred power of the DC/DC converter are simplified to an analytically calculable form, where the fundamental curve form is not changed. Thus, the results are qualitatively transferable to the analyzed systems and help to understand the results from the full model applied on the following pages. The assumed PV-generators characteristic:

$$P_{PV}(U_{in}) = A \left( U_{MPP}^2 - (U_{in} - U_{MPP})^2 \right) \quad \text{with } A > 0 \quad (2)$$

shows one MPP, no power at zero voltage and an open circuit voltage of twice the MPP voltage. The DC/DC converters equation:

Table 1. Overview of different DC/DC converters

| Topology  | Transferred Power: $P_{DC/DC}$   | Comments regarding controllability  |
|---|--|---|
| <p>Single Phase Single Active Bridge (SAB1)</p> | $\frac{U_{in} U'_{dc}}{f \cdot L} \cdot \left( \frac{\beta}{4\pi} - \frac{1}{8} \frac{U'_{dc}{}^2}{U_{in}^2} - \frac{1}{8} \frac{\beta^2}{\pi^2} \right)$  | Transformers effective input voltage adapted with $\beta$ , buck operation, [4] [5]                                   |
| <p>Single Phase Dual Active Bridge (DAB1)</p>   | $\frac{U_{in} U'_{dc}}{f \cdot L} \cdot \frac{\phi}{2\pi} \left( 1 - \frac{\phi}{\pi} \right)$   | Phase shifted operation with $\phi$ as parameter, buck boost operation, [4] [5]                                       |
| <p>Three Phase Single Active Bridge (SAB3)</p>  | $\frac{U_{in} U'_{dc}}{f \cdot L} \cdot \frac{1}{9} \left( 1 - \frac{U'_{dc}{}^2}{U_{in}^2} \right), \quad U_{in} \leq 2U'_{dc}$ $\frac{U_{in} U'_{dc}}{f \cdot L} \cdot \frac{1}{72} \left( 7 - 4 \frac{U'_{dc}{}^2}{U_{in}^2} \right), \quad U_{in} \geq 2U'_{dc}$                     | Buck operation, same theory like three phase dual active bridge, with a $\phi$ determined by the operating point, [4] |
| <p>Three Phase Dual Active Bridge (DAB3)</p>    | $\frac{U_{in} U'_{dc}}{f \cdot L} \cdot \frac{\phi}{2\pi} \left( \frac{2}{3} - \frac{\phi}{2\pi} \right), \quad \phi \leq \frac{\pi}{3}$ $\frac{U_{in} U'_{dc}}{f \cdot L} \cdot \left( \frac{\phi}{2\pi} - \frac{\phi^2}{2\pi^2} - \frac{1}{36} \right), \quad \phi \geq \frac{\pi}{3}$ | Phase shifted operation with $\phi$ as parameter, buck boost operation, [4] [5]                                       |

$$P_{DC/DC}(U_{in}) = C \frac{U_{in}}{f} \quad \text{with } C > 0 \quad (3)$$

is simplified regarding Table I. Each of the equations has the frequency in the denominator. The output voltage is fixed by the DC/AC inverter. For the input voltage it was proven for each topology in table I that the voltage is increasing with power. A linear simplification is assumed. Additional possibilities for control are neglected in this step.

Inserting equations (2) and (3) into each other, either power or voltage can be determined depending on the converters switching frequency, which is the only possibility to control the converter in its simplified form:

$$U_{in}(f) = 2U_{MPP} - \frac{C}{A} \frac{1}{f} \quad (4)$$

$$P(f) = 2C \frac{U_{MPP}}{f} - \frac{C^2}{A} \frac{1}{f^2} \quad (5)$$

Figure 3 is a plot of the operating points, resulting from equations (4) and (5), of the idealized system PV-module and DC/DC converter.

The ability of performing MPPT by variation of frequency is shown in the same plot. By changing the frequency only one MPP of the system PV-generator and DC/DC converter exists, which is not an obvious result and is different in other topologies not mentioned in table I. Such calculations applied on real converters allow to determine the necessary margin in which the frequency has to be adjustable for the different operating points.

#### 4. ANALYSIS OF THE FULL SYSTEM

The idealized approach is implemented in the mathematics tool Matlab for the full model: PV-generator with its curves A to E from Figure 2 and the different DC/DC converters with the equations given in Table 1. The implementation allows to choose the transformer's turns ratio  $U_{dc}/U'_{dc}$  and its leakage inductance  $L$ . The following sections show the numerically determined results, keeping  $L$  as a variable parameter and setting  $U'_{dc}$  to different constant values. (With the turns ratio constant and  $U_{dc}$  controlled to a constant value by the inverter).

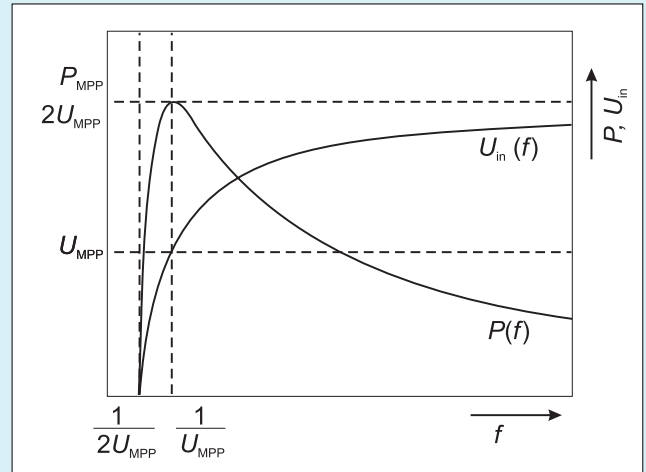


Fig. 3. Characteristics of the Idealized System PV-Generator and DC/DC Converter with  $A = C = 1$

For the purpose of a didactic explanation, the topologies with the lowest number of controllable parameters are qualified first, starting with SAB3.

#### 4.1. Three Phase Single Active Bridge (SAB3)

Since the single active bridges are buck converters,  $U_{dc}$  has to be chosen smaller than the minimum MPP voltage, being 26 V (cmp. Fig. 2).

The equivalent result for SAB3 is shown in Figure 4 (also cmp. Fig. 3). It can be seen that each curve has exactly one maximum, proving the controllability by frequency, which is the only adjustable parameter during operation in SAB3. The results of the calculations also help to design the converter. The maximum power points of the curves B and C determine the maximum frequency ratio between minimum and maximum frequency, where leakage inductance  $L$  is still a variable parameter. In order to determine this frequency ratio, the design parameter  $U'_{dc}$  has to be taken into account (cmp. the different results in Fig. 4).

For the reason of readability only the MPP-operating points of curves A to E, assumed that they are tracked, are now analyzed. Figure 5 shows the necessary frequency — together with the design parameter leakage inductance  $L$  — depending on  $U'_{dc}$ .

As already mentioned before, the curves B and C determine the maximum frequency ratio which has to be adjustable for MPP tracking. In Figure 6 this ratio is plotted depending on  $U'_{dc}$ .

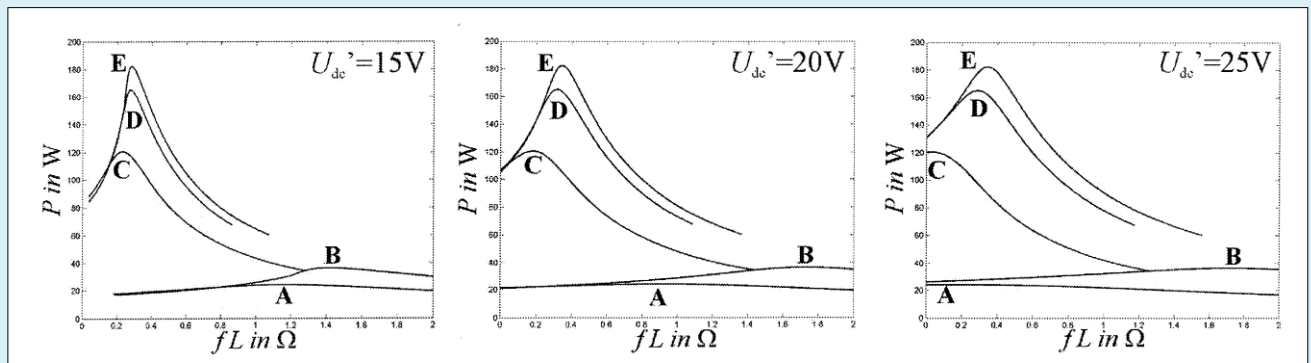


Fig. 4. Characteristic of the System PV-Generator with SAB3

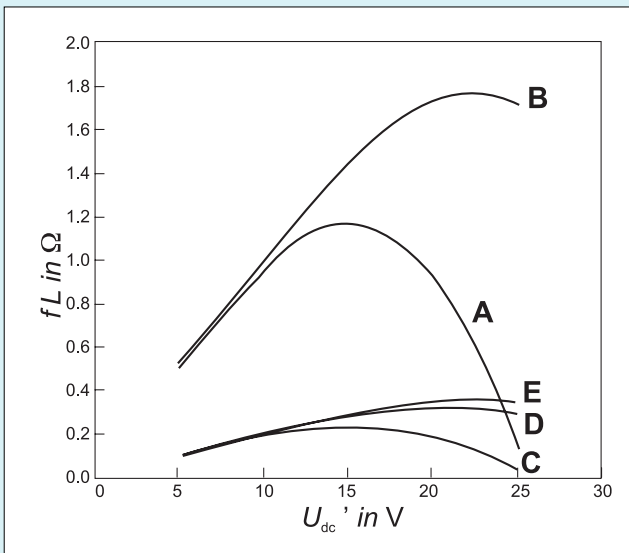


Fig. 5. Necessary  $fL$  Product for MPP

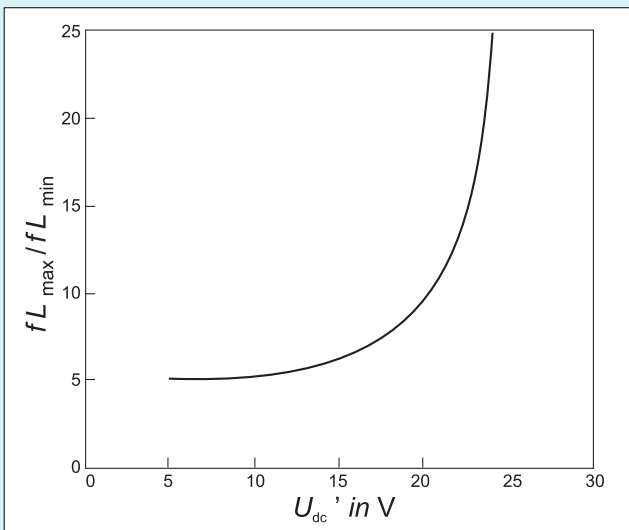


Fig. 6. Necessary Adjustable Frequency Ratio for SAB3

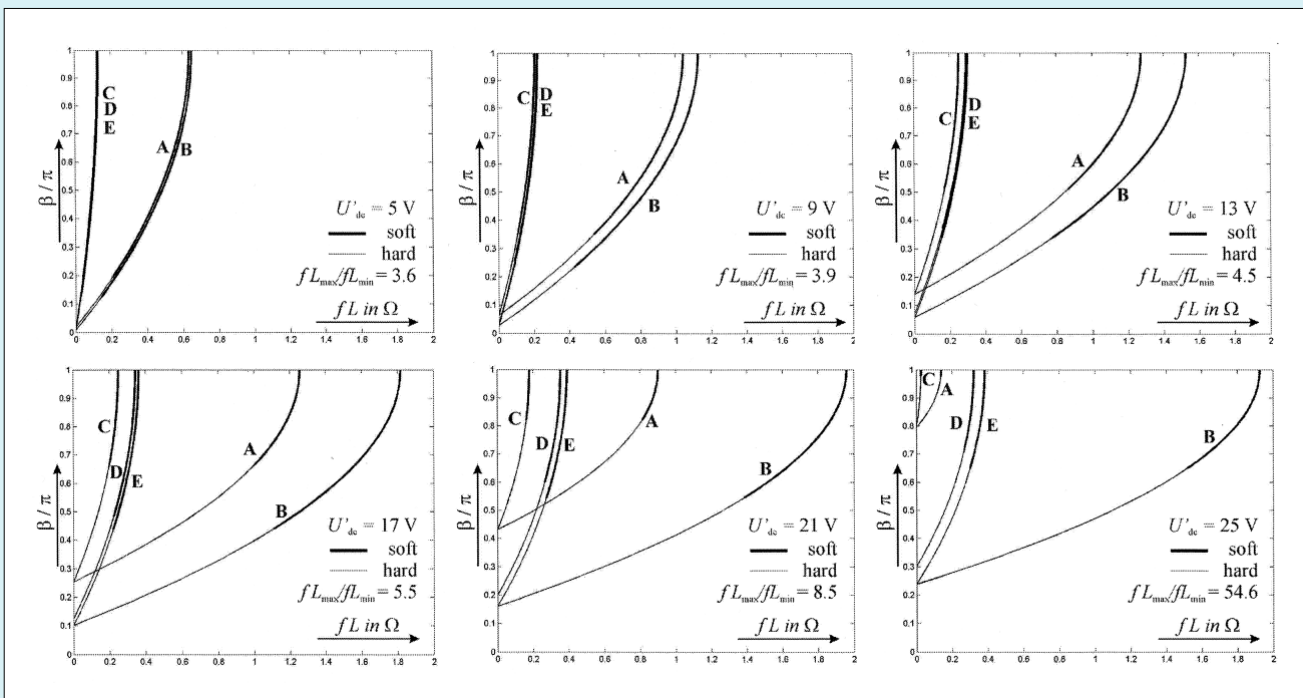


Fig. 7. Results for the System SAB1 with PV-generator

With decreasing  $U'_{dc}$  the necessary frequency ratio also decreases, but at the same time the transformer turn-ratio increases resulting in increased transformer losses. Designing such a SAB3 then becomes a tradeoff in choosing  $U'_{dc}$ . For the PV-generator presented in figure 2  $U'_{dc}=15$  V would be suitable, because lower values do not have a big advantage in terms of a lower frequency ratio.

#### 4.2. One Phase Single Active Bridge (SAB1)

As already mentioned for SAB3, the SAB1 is also a buck converter. Thus, it is showing a maximum voltage  $U'_{dc}$  smaller than the minimum MPP voltage, being 26 V (cmp. Fig. 2).

The mathematic tool shows the controllability for SAB1 similar to the Figures 3 and 4, but the corresponding figure for SAB1 is not presented again.

SAB1 has one additional control parameter, i.e. the phase shift  $\beta$  between the two input half bridges both operating with a duty cycle of 50% [4, 5]. Thus, the effective input voltage of the converter could be changed by controlling the phase shift  $\beta$ .

In Figure 7 the MPP operating points A to E are plotted for different combinations of the control parameters  $\beta$  and  $f$ . A variation of the curves can be seen for different values of the design parameter  $U'_{dc}$ . As additional information it is pointed out, whether the specific operating point of the bridge provides soft switching or not.

In the design of such a DC/DC converter a strategy to answer the following question has to be defined: Which combination of phase shift and frequency is applied to operate the system? Figure 7 shows a variety of possibilities.

The maximum frequency ratio is requested to be low, since transformer utilization increases for most operating points. Furthermore, the circuit design becomes much easier. For PV-applications a high efficiency is essential, thus only soft switching operating points are taken into account. Hence, the phase shift  $\beta$  is chosen in such a way that the frequency

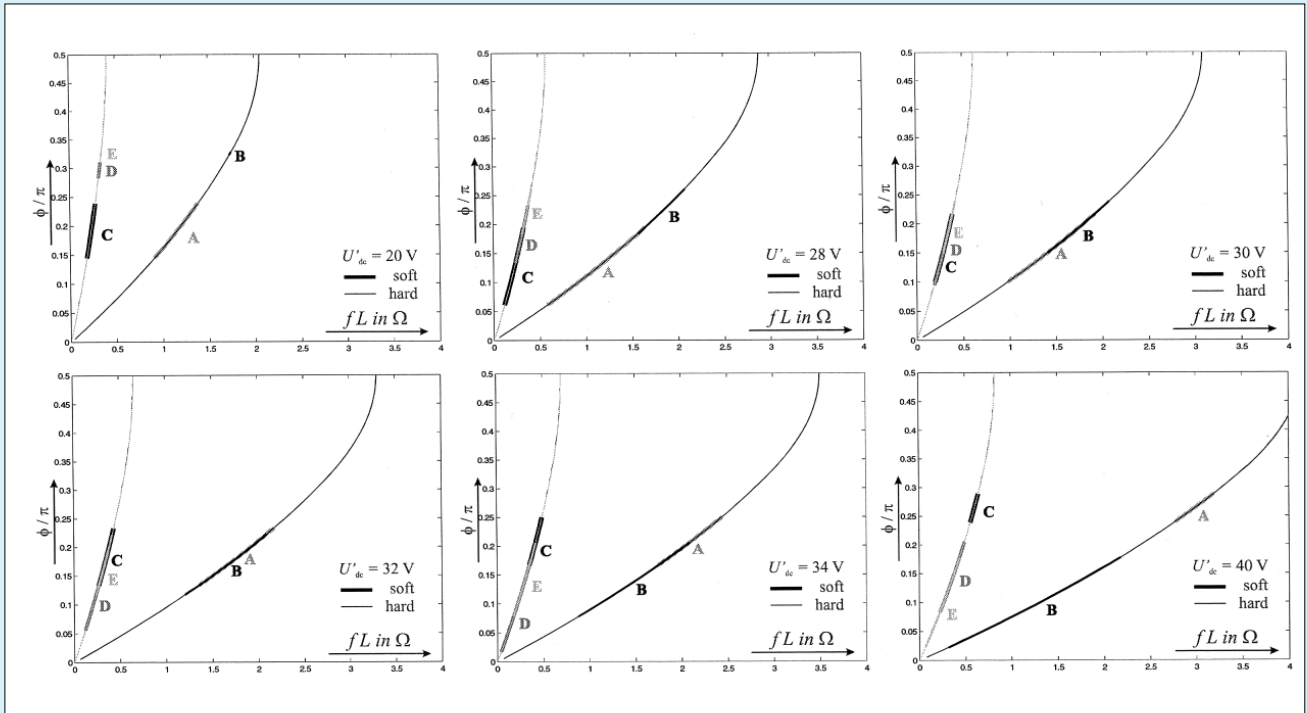


Fig. 8. Results for the System DAB3 with PV-generator

ratio is minimum. Within this choice of  $\beta$  the boundary condition of ensuring soft switching is taken into account. Compared to Figure 7, the lower frequency boundary is defined by curve C at maximum phase shift of  $\beta/\pi = 1$ . The upper frequency boundary is defined by the operating points of the curves A or B respectively, depending on which curve needs the higher frequency at minimum phase shift to enable soft switching

As a result the necessary frequency ratio is itemized for different values of the design parameter  $U'_{dc}$ . This frequency ratio increases monotonously with  $U'_{dc}$ , as it could already be seen for SAB3 (cmp. Fig. 6). Comparing the numbers in Figure 7, a good tradeoff for choosing  $U'_{dc}$  is a value of about 15 V.

One strategy to operate the bridge when tracking the maximum power point would be to either vary frequency at maximum  $b$  or vary phase shift at maximum  $f$ . Hence, all operating points can be realized ensuring soft switching.

### 4.3. Three Phase Dual Active Bridge (DAB3)

In contrast to the analyzed systems with single active bridge converters the DAB3 is a buck-boost converter. Hence, for the choice of the design parameter  $U'_{dc}$  the upper value is not limited.

The mathematic tool shows the controllability for DAB3 similar as in the previous systems, but the corresponding figure to the Figures 3 and 4 is not presented again.

DAB3 has one control parameter in addition to switching frequency  $f$ , i.e. the phase shift  $\phi$  between the input and the output bridge each consisting of three half bridges. With the equations given in table I,  $\phi$  varies between zero and  $90^\circ$ , since only unidirectional power flow is taken into account and higher values of  $f$  let decrease power again [4, 5].

In Figure 8, the MPP operating points A to E are plotted as curves for different combinations of the control parameters

phase shift  $\phi$  and frequency  $f$ . For example curve D shows the operating point under standard test conditions of the PV-generator. It can be realized in different ways by the converter. Figure 8 shows in contrast to previous results, that the curves A and B and the curves C, D and E are very close to each other. This is reasoned by very similar values of  $P_{MPP} / U_{in\_MPP}$  for the similar curves. Regarding table I, DAB3 is then only determined by  $f$  and  $\phi$  and has no additional dependencies on the input voltage  $U_{in}$  like other topologies. Additionally there is also no complex but only a linear dependency on the design parameter  $U'_{dc}$ . Thus, the curves in the different diagrams in Figure 8 are the same but only scaled on the  $fL$  axis by the factor of  $U'_{dc}$ .

Hence, the question arises: Why is the result in Figure 8 not plotted in one single Figure with the  $fL$  axis containing the design parameter  $U'_{dc}$ ? The results are plotted for 20, 28, 30, 32, 34 and 40 V for the purpose of visualizing the boundary between soft and hard switching, depending on  $U'_{dc}$ . In case of buck operation, hard switching of the output bridge has to be avoided, the same applies to the input bridge in case of boost operation.

In Figure 8 the soft switching operating points of the DC/DC converter are indicated. The converter shows the widest ranges of soft switching operating points, when  $U'_{dc}$  is chosen to a value similar to  $U_{in}$  (cmp. Fig. 8 for  $U'_{dc} = 32$  V and Fig. 2).

Analogue to the control of SAB1 a strategy of applying combinations of control parameters has to be defined. As mentioned before, the strategy has to ensure a low necessary frequency ratio and soft switching in order to keep the efficiency high. Figure 8 shows different possibilities: With a sophisticated controller managing a high computation effort the soft switching boundaries could be calculated and the frequency ratio could be minimized. Alternatively, if  $U'_{dc} = 32$  V is chosen, all operation points are soft switching

for a fixed  $\phi / \pi = 0.17$  (cmp. Fig. 8). Thus, only frequency needs to be controlled. In this specific example a frequency ratio of 5 is necessary (cmp. Fig. 8).

## 5. CONCLUSION

This paper describes the control of a module integrated converter for photovoltaic applications with focus on the system PV-generator and DC/DC converter. Basic requirements for the ability of maximum power point tracking are analyzed analytically and verified for real systems by means of a mathematic model. Applying this tool it was qualified, that the different systems are controllable. Design rules based on the calculations have been presented for all analyzed systems.

## REFERENCES

1. Meinhardt M.: *State of the Art and Future of power Electronics for the use in Grid-tied PV-Systems — The Industrial Perspective*. Tutorial on Power Electronics for Regenerative Energy within the 35th Annual IEEE Power Electronics Specialists Conference, 2004.
2. Photon – Das Solarstrom-Magazin: *SMA präsentiert kleinen Zentralwechselrichter mit 98 Prozent Wirkungsgrad*. German magazine, July 2005.
3. Bartz T., Rigbers K., De Doncker R.W.: *Modulintegrierter Wechselrichter mit erhöhter Lebensdauer*. 18 Symposium Photovoltaische Solarenergie, Staffelstein, 12.-14. März 2003.
4. De Doncker R.W., Divan D.M., Kheraluwala M.H.: *A Three-Phase Soft-Switched High-Power-Density DC/DC Converter for High-Power Applications*. IEEE transactions on industry Applications, 1991, 27.
5. Kheraluwala M.H.: *High Power High Frequency DC/DC Converter*. Dissertation Thesis, University of Wisconsin - Madison, 1990.



### Christian P. Dick

was born in Limburg a.d. Lahn, Germany in 1977. He studied Electrical Engineering at RWTH Aachen University, Germany and received his Diploma degree in May 2004. In July 2004 he joined the Institute for Power Electronics and Electrical Drives (ISEA) of Prof. De Doncker at RWTH Aachen University as a research associate. His main research interests are power electronics, i.e the integration of power

electronic circuits in PCB's and the utilization of renewable energy.

Address:

Institute for Power Electronics and Electrical Drives (ISEA)

RWTH Aachen University in Germany

Jaegerstrasse 17–19, 52066 Aachen, Germany

e-mail: di@isea.rwth-aachen.de



### Klaus Rigbers

was born in Delmenhorst, Germany in 1976. He received his Dipl.-Ing. degree from the Technical University Braunschweig, Germany in 2002. In 2002 he joined the Institute for Power Electronics and Electrical Drives (ISEA) at RWTH Aachen University as research associate. His main research interests are all aspects of high efficient low and medium power converters.

Address:

Institute for Power Electronics and Electrical Drives (ISEA)

RWTH Aachen University in Germany

Jaegerstrasse 17–19, 52066 Aachen, Germany

e-mail: ri@isea.rwth-aachen.de



### Harald Radermacher

was born in Stolberg, Germany, in 1973. He studied Electrical Engineering at RWTH Aachen University, Germany and received his Diploma degree in April 2000. In May 2000 he joined the Institute for Power Electronics and Electrical Drives (ISEA) of Prof. De Doncker at RWTH Aachen University as a research associate. His main research interests are power electronics, i.e single phase systems, power factor

correction and DSP control.

Address:

e-mail: rm@isea.rwth-aachen.de



### Rik W. De Doncker

was born in Leuven, Belgium, in 1958. He received his degree of Doctor in Electrical Engineering from the Katholieke Universiteit Leuven, Belgium in 1986. During 1987 he was appointed Visiting Associate Professor at the University of Wisconsin, Madison. In Dec. 1989, he joined the General Electric Company at the Corporate Research and Development Center, Schenectady, NY. In 1994, he joined Silicon Power

Corporation (formerly GE-SPCO) as Vice President Technology. Since Oct. 1996 he is professor at RWTH Aachen University, where he leads the Institute for Power Electronics and Electrical Drives. He is an IEEE Fellow and for 2005/2006 the President of the IEEE Power Electronics Society (PELS).

Address:

Institute for Power Electronics and Electrical Drives (ISEA)

RWTH Aachen University in Germany

Jaegerstrasse 17–19, 52066 Aachen, Germany

e-mail: dd@isea.rwth-aachen.de